

# Calculations of Electron Inelastic Mean Free Paths (IMFPs)

## IV. Evaluation of Calculated IMFPs and of the Predictive IMFP Formula TPP-2 for Electron Energies between 50 and 2000 eV

S. Tanuma

Analysis Research Center, Nippon Mining Company, Ltd., 3-17-35 Niizo-Minami, Toda, Saitama 335, Japan

C. J. Powell and D. R. Penn

National Institute of Standards and Technology, Gaithersburg, MD 20899, USA

We have made additional evaluations of the electron inelastic mean free paths (IMFPs) and of the predictive IMFP formula TPP-2 presented in papers II and III of this series. Comparisons have been made with other formulae for the IMFPs and electron attenuation lengths (ALs). We find substantial differences between our IMFP results for 27 elements and 15 inorganic compounds and the AL formulae of Seah and Dench; these differences include different dependences on electron energy and on material parameters. We present IMFP calculations for  $\text{Al}_2\text{O}_3$  and GaAs from TPP-2 in which each parameter of the formula is varied in some physically reasonable range about the true value for each compound; these results show the sensitivity of the computed IMFPs to the choices of parameter values. Finally, we give a summary of sources of uncertainty in the IMFP algorithm, in the experimental optical data from which IMFPs are calculated, and of the TPP-2 formula. We conclude that TPP-2 is robust and useful for predicting IMFPs for electron energies and material parameter values in ranges for which the formula was developed and tested.

### INTRODUCTION

We have recently reported new calculations of inelastic mean free paths (IMFPs) for 50–2000 eV electrons in a group of 27 elements and a group of 15 inorganic compounds.<sup>1,2</sup> These calculations were based on an algorithm due to Penn,<sup>3</sup> which combines experimental optical data for each material (to describe the dependence of the inelastic scattering probability on energy loss), and the theoretical Lindhard dielectric function<sup>4</sup> (to describe the dependence of the scattering probability on momentum transfer). We fitted the calculated IMFPs for the group of elements to a modified form of the Bethe equation<sup>5</sup> for inelastic electron scattering in matter and found that the four parameters in this equation could be related empirically to several material parameters (atomic weight, density, number of valence electrons per atom and bandgap energy). The resulting equation, to be referred to as TPP-2, gave IMFP values for the 27 elements that differed from those initially calculated by 13% RMS (root mean square). In contrast, the corresponding RMS difference between IMFP values calculated for the group of compounds and those determined from TPP-2 was much larger, ~23%. The deviation for each compound correlated, however, with uncertainties of the optical data from which the IMFPs were calculated. As a result, we concluded that IMFPs obtained from TPP-2 for these compounds were more reliable than those calculated from the optical data.

In this paper, we present the results of other tests that we have made to assess the reliability of the IMFP predictive formula TPP-2. We are interested particularly in

the accuracy of IMFPs determined from TPP-2 and the reliability of the dependences on electron energy and on material parameters. We also compare TPP-2 with other formulae that have been proposed to represent IMFPs and electron attenuation lengths (ALs).<sup>6</sup> Comments are given on comparative tests of the IMFP and AL formulae for quantitative surface analyses by Auger electron spectroscopy (AES) and x-ray photoelectron spectroscopy (XPS). We then present tests of the sensitivity of IMFPs computed from TPP-2 to the choice of parameters for two compounds,  $\text{Al}_2\text{O}_3$  and GaAs. Finally, we discuss sources of uncertainty in the IMFP values for application in AES and XPS, uncertainties of the optical data used in our IMFP calculations, and uncertainties of the TPP-2 predictive formula.

### IMFP VALUES

We will analyse in this paper IMFPs calculated from experimental optical data using the Penn algorithm for the group of 27 elements<sup>1</sup> (C, Mg, Al, Si, Ti, V, Cr, Fe, Ni, Cu, Y, Zr, Nb, Mo, Ru, Rh, Pd, Ag, Hf, Ta, W, Re, Os, Ir, Pt, Au and Bi) and IMFPs calculated from optical data and from the TPP-2 formula for the group of 15 inorganic compounds<sup>2</sup> ( $\text{Al}_2\text{O}_3$ , GaAs, GaP, InAs, InP, InSb, KCl, LiF, NaCl, PbS, PbTe, SiC,  $\text{Si}_3\text{N}_4$ ,  $\text{SiO}_2$  and ZnS). These materials were selected because the optical data needed were conveniently available.<sup>1,2</sup>

The TPP-2 formula<sup>1</sup> is

$$\lambda = E / \{ E_p^2 [\beta \ln(\gamma E) - (C/E) + (D/E^2)] \} \quad (1)$$

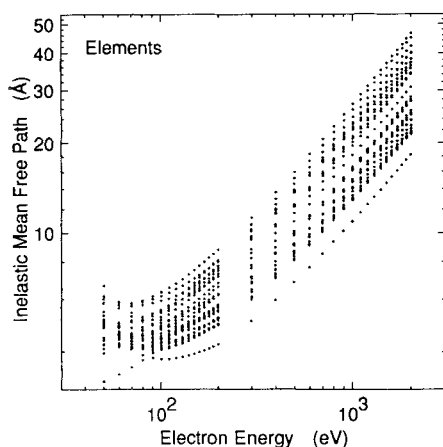


**Figure 1.** Summary plot of calculated IMFPs from Ref. 1 for the group of 27 elements as a function of electron energy.

where  $\lambda$  is the IMFP (in Å),  $E$  is the electron energy (in eV),  $E_p = 28.8 (N_v \rho / M)^{1/2}$  is the free-electron plasmon energy (in eV),  $\rho$  is the density (in g cm<sup>-3</sup>),  $N_v$  is the number of valence electrons per atom (for elements) or molecule (for compounds) and  $M$  is the atomic or molecular weight. The terms  $\beta$ ,  $\gamma$ ,  $C$  and  $D$  are parameters given by

$$\beta = -0.0216 + 0.944/(E_p^2 + E_g^2)^{1/2} + 7.39 \times 10^{-4} \rho \quad (2)$$

$$\gamma = 0.191 \rho^{-0.50} \quad (3)$$

$$C = 1.97 - 0.91U \quad (4)$$

$$D = 53.4 - 20.8U \quad (5)$$

$$U = N_v \rho / M = E_p^2 / 829.4 \quad (6)$$

and  $E_g$  is the bandgap energy (in eV) for non-conductors.

Figure 1 is a summary plot showing the calculated IMFPs for the group of elements versus electron energy over the 50–2000 eV range. This plot shows the overall trends in the IMFP variations with energy for this group of materials and particularly shows the differences in the shapes of the IMFP–energy curves in the 50–200 eV range.<sup>1</sup> The Penn algorithm<sup>3</sup> is believed to be useful for energies down to 50 eV (additional discussion on this point is given below) but IMFP estimates at lower energies show the expected IMFP increase.<sup>1</sup>

Figure 1 also indicates the range in IMFP values found for these 27 elements at any one energy. Such ranges should not be regarded as limiting values since other elements may have smaller or larger IMFPs. For example, the alkali metals have appreciably lower densities than the elements considered here and their IMFPs would be expected to be larger (at any one energy) than those shown in Fig. 1.<sup>7</sup> Nevertheless, Fig. 1 indicates that the range in the IMFP values at any energy for the present group of elements varies between a factor of 1.7 and a factor of 2.6.

Figure 2 shows IMFP data as a function of energy for the group of inorganic compounds. Figure 2(a) is a plot of IMFPs calculated using the Penn algorithm from experimental optical (as was done for the elemental IMFPs in Fig. 1). There were, however, significant

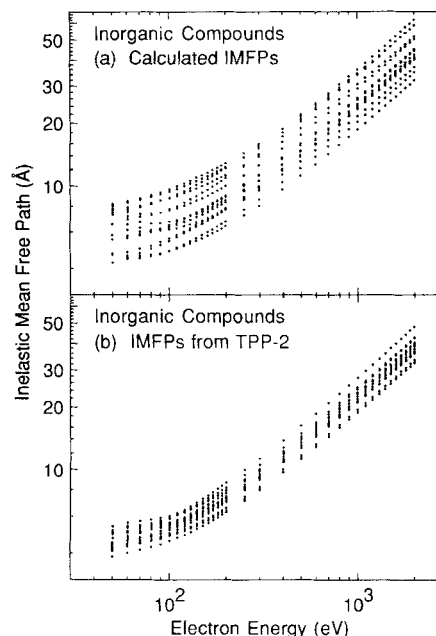


**Figure 2.** Summary plot of IMFPs calculated (a) from experimental optical data and (b) from TPP-2 (Ref. 2) for the group of 15 inorganic compounds as a function of electron energy.

errors found in the optical data for many of the inorganic compounds based on checks with optical sum rules.<sup>2</sup> We therefore suggested that IMFPs calculated from TPP-2 would be more reliable than those directly calculated from the optical data. Figure 2(b) shows IMFPs calculated from TPP-2 for the 15 inorganic compounds; these values show the same general dependence on electron energy as the IMFPs in Fig. 2(a) but the range at any one energy is less. The range between the largest and smallest IMFP at any energy [Fig. 2(a)] is about a factor of 2 whereas the corresponding range in Fig. 2(b) is a factor of  $\sim 1.4$ . There are also variations in the shapes of the IMFP–energy data for energies between 50 and 200 eV in Fig. 2(a) but such variations are less pronounced in Fig. 2(b).

Figure 3 shows plots of the ratios of IMFPs calculated from TPP-2 to IMFPs calculated from optical data for the group of elements [Fig. 3(a)] and the group of compounds [Fig. 3(b)] as a function of electron energy. Ideally, these ratios should not change with energy and should be close to unity. For most materials, the ratios are nearly constant with energy for energies above 200 eV but there are often substantial changes at lower energies. The scatter of the points in Fig. 3(a) is an indication of the degree of success of TPP-2 in representing the IMFP dependences on material parameters; the root-mean-square (RMS) deviation of the points in Fig. 3(a) from unity is  $\sim 13\%$ , as reported previously.<sup>1</sup> The RMS deviation of the points in Fig. 3(b) from unity is  $\sim 23\%$ , but this larger deviation is believed to be due to deficiencies in the optical data used for the IMFP calculations.<sup>2</sup> Most of the ratios in Fig. 3(b) are less than unity, and there is a correlation between the average RMS differences in the comparisons of IMFP values calculated for each compound with IMFPs from TPP-2 and the average of the errors in the optical data for the corresponding compound as revealed by two sum rules.<sup>2</sup>

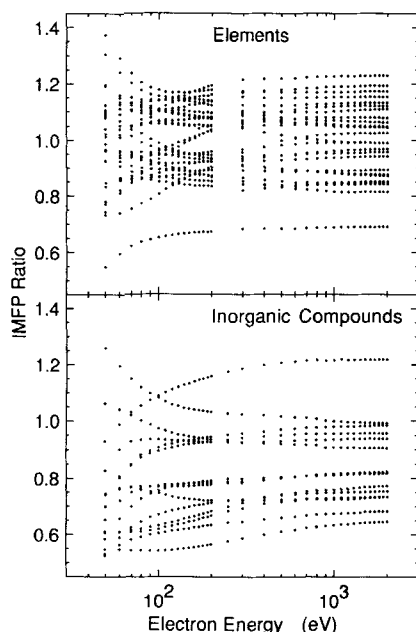


**Figure 3.** Ratio of IMFPs calculated from TPP-2 to IMFPs calculated from optical data as a function of electron energy for (a) the group of 27 elements and (b) the group of 15 inorganic compounds.

### IMFP DEPENDENCES ON ELECTRON ENERGY AND ON MATERIAL PARAMETERS

We compare here our IMFP results and TPP-2 with equations that have been proposed for the representation of ALs and IMFPs. Our IMFPs have been derived in a consistent way with the same algorithm.<sup>3</sup> Although there are approximations in the theory, to be discussed further below, which lead to uncertainties in the calculated IMFPs, the main source of variability in the evaluation of IMFPs for a given material arises from uncertainties in the available experimental optical data used in the calculations.<sup>1,2</sup> It is, in fact, convenient and appropriate to use our set of calculated IMFPs for the groups of elements and compounds for comparisons with AL and IMFP equations on account of the high degree of precision and internal consistency of our IMFPs; this level of precision and internal consistency is superior to that for the available AL data, which generally have substantial uncertainties.<sup>6</sup>

#### The AL equation of Wagner, Davis and Riggs

Our first comparison is with the equation proposed by Wagner *et al.*<sup>8</sup> to analyse the dependences of measured ALs on electron energy

$$\lambda_{AL} = kE^m \quad (7)$$

where  $\lambda_{AL}$  is the AL expressed in Å,  $E$  is expressed in eV and  $k$  and  $m$  are parameters. Wagner *et al.* examined sets of AL data as a function of energy for a number of materials that had each been determined in a single laboratory. They found that  $m$  was material-dependent

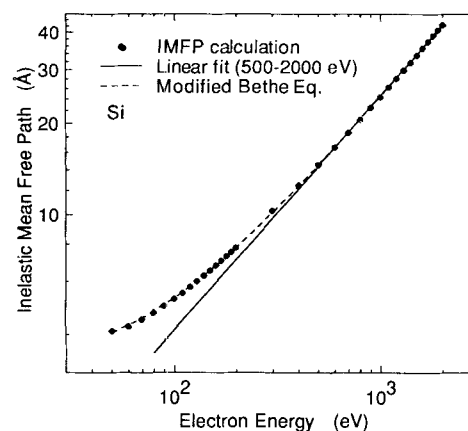


**Figure 4.** Plot of calculated IMFPs for silicon (solid circles) as a function of electron energy on logarithmic scales. The solid line is a fit of Eqn (7) to the calculated IMFPs over the 500–2000 eV range. The dashed line is a fit of the modified Bethe equation [Eqn (3)] to the calculated IMFPs over the 50–2000 eV range with the four parameters  $\beta$ ,  $\gamma$ ,  $C$  and  $D$  allowed to vary (Ref. 1).

(as was  $k$ ) and ranged from 0.54 to 0.81. Generally, similar results have been reported by others.<sup>9–11</sup> Equation (7) has also been used for similar analyses of calculated IMFPs.<sup>12</sup> Although there is no known physical basis for Eqn (7), it is a relatively simple and convenient means for expressing AL and IMFP dependences on electron energy.

We have fitted Eqn (7) to our calculated IMFPs for the group of 27 elements<sup>1</sup> and to IMFPs calculated from optical data and from TPP-2 for the group of 15 compounds.<sup>2</sup> The electron energy range over which we could obtain satisfactory fits varied somewhat with material but we arbitrarily decided to report fits here for the 500–2000 eV range. The RMS deviations in the fits for each solid varied between 0.35% and 0.87%, while the largest deviation (always at 500 eV) varied between 0.8% and 2.1%.

Examples of the fits of Eqn (7) to our IMFPs for Si and Pt are shown in Figs 4 and 5, respectively. It is clear from Figs 4 and 5 that Eqn (7) is unsatisfactory for energies below  $\sim 500$  eV. The dashed lines show fits<sup>1</sup> of the modified Bethe equation [Eqn (1) with the param-

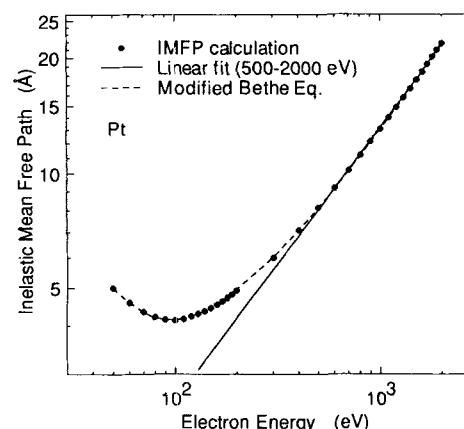


**Figure 5.** An IMFP plot for platinum as a function of electron energy; see caption to Fig. 4.

eters  $\beta$ ,  $\gamma$ ,  $C$  and  $D$  allowed to vary] to the calculated IMFPs; the fits are seen to be clearly superior to those found with Eqn (7). Equation (1) has four parameters but the two-parameter predictive formula TPP is useful over the 200–2000 eV range,<sup>13</sup> and this latter equation would also be superior to Eqn (7). The principal limitation of Eqn (7) is the curvature in the log-log plots of both ALs and IMFPs as a function of energy;<sup>6,8,9,12</sup> this limitation was obviated to some extent by Ashley and Tung,<sup>12</sup> who made separate fits with Eqn (7) over the 200–400 eV, 400–2000 eV and 2000–10 000 eV energy ranges.

Tables 1 and 2 list values of the parameters  $k$  and  $m$  determined in the fits with Eqn (7) for each material. The factor  $k$  varies between 0.0804 and 0.132 Å for the group of elements and between 0.0936 and 0.235 Å for the group of compounds (the exact range depending for the compounds on the IMFP data set being analysed). The exponent  $m$  similarly varies between 0.706 and 0.789 for the group of elements and between 0.725 and 0.787 for the group of compounds.

Although Eqn (7) has no direct physical basis, the functional dependence of  $\lambda_{AL}$  on energy is similar to that of Eqn (1) for energies between 500 and 2000 eV, as shown in Figs 4 and 5. For this energy range, we can ignore the second and third terms of Eqn (1) so that

$$\lambda \approx E/\beta E_p^2 (\ln \gamma + \ln E) \quad (8)$$

If  $\ln \gamma$  is small compared to  $\ln E$ , Eqn (7) provides a good representation of the dependence of  $E/\ln E$  on

**Table 1. Values of the parameters  $k$  and  $m$  in the fits of Eqn (7) to IMFPs calculated from experimental optical data for 27 elements (Ref. 1) over the electron energy range 500–2000 eV**

Element	$k$ (Å)	$m$
C	0.129	0.775
Mg	0.112	0.789
Al	0.0920	0.777
Si	0.116	0.775
Ti	0.104	0.783
V	0.0998	0.775
Cr	0.0858	0.763
Fe	0.0897	0.753
Ni	0.0942	0.734
Cu	0.107	0.729
Y	0.117	0.768
Zr	0.104	0.768
Nb	0.132	0.745
Mo	0.0941	0.748
Ru	0.0843	0.752
Rh	0.0812	0.747
Pd	0.104	0.748
Ag	0.0924	0.730
Hf	0.156	0.719
Ta	0.104	0.720
W	0.0958	0.716
Re	0.0804	0.713
Os	0.0990	0.706
Ir	0.104	0.708
Pt	0.0956	0.714
Au	0.0951	0.713
Bi	0.118	0.746

**Table 2. Values of the parameters  $k$  and  $m$  in the fits of Eqn (7) to IMFPs calculated from experimental optical data and from TPP-2 for 15 inorganic compounds (Ref. 2) over the electron energy range 500–2000 eV**

Compound	IMFPs from optical data		IMFPs from TPP-2	
	$k$ (Å)	$m$	$k$ (Å)	$m$
Al <sub>2</sub> O <sub>3</sub>	0.122	0.750	0.112	0.760
GaAs	0.235	0.725	0.114	0.763
GaP	0.144	0.755	0.106	0.769
InAs	0.192	0.736	0.121	0.763
InP	0.0977	0.761	0.114	0.767
InSb	0.196	0.749	0.129	0.763
KCl	0.169	0.769	0.122	0.787
LiF	0.127	0.764	0.118	0.768
NaCl	0.192	0.760	0.110	0.783
PbS	0.121	0.765	0.119	0.753
PbTe	0.114	0.771	0.130	0.753
SiC	0.104	0.764	0.0936	0.770
Si <sub>3</sub> N <sub>4</sub>	0.136	0.751	0.0993	0.766
SiO <sub>2</sub>	0.150	0.764	0.103	0.777
ZnS	0.145	0.752	0.0986	0.763

energy [as then expected from Eqn (8)] in the 500–2000 eV range with  $m = 0.856$ . For our materials,  $\ln \gamma$  is not small compared to  $\ln E$  and the  $\ln \gamma$  term in Eqn (8) can be regarded as both the reason for the lower values found for the parameter  $m$  and the source of the variations found in  $m$  from material to material (Tables 1 and 2). The value of  $m$  is thus related to  $\ln \gamma$ , which is expected to depend on how the differential cross-section for inelastic scattering varies as a function of energy loss.<sup>14</sup> Since there is no physical basis for Eqn (7), it is not possible to make direct predictions as to how the parameters  $k$  and  $m$  should vary from one material to another. Nevertheless, it appears from Tables 1 and 2 that  $m = 0.75 \pm 0.03$  (one standard deviation) is a reasonable approximation for this group of materials over the 500–2000 eV range.

We note that our determination of the values of  $m$  in Tables 1 and 2 pertain to the use of Eqn (7) for describing IMFPs; the corresponding values of  $m$  for ALs could be slightly larger or smaller than for the corresponding IMFPs.<sup>10</sup>

#### IMFP equations of Szajman *et al.* and of Ashley

Szajman *et al.*<sup>15</sup> have reported a general IMFP equation based on an expression for the IMFP  $\lambda_v$  due only to valence-electron excitations derived by Szajman and Leckey.<sup>16</sup> After consideration of inelastic scattering by core-electron excitations, Szajman *et al.*<sup>15</sup> find the following approximate IMFP formula (for electron energies of  $> 300$  eV)

$$\lambda \approx 1.8 \bar{E} E^{3/4} / E_p^2 \quad (\text{in Å}) \quad (9)$$

where  $\bar{E}$  is the centroid in the energy-loss function. For insulators and semiconductors, Szajman *et al.* indicate that

$$\bar{E} = E_p + E_g \quad (10)$$

For free-electron-like solids where  $\bar{E} \approx E_p$ , Eqn (10) becomes

$$\lambda \approx 1.8E^{3/4}/E_p = 0.0625E^{3/4}(A/\rho N_v)^{1/2} \quad (\text{in } \text{\AA}) \quad (11)$$

Ashley<sup>17</sup> has calculated  $\lambda_v$  for organic solids. For electron energies between 600 and 2000 eV, his result can be simplified to

$$\lambda_v \approx 1.88\bar{E}E^{0.78}/E_p^2 \quad (\text{in } \text{\AA}) \quad (12)$$

If it is again assumed that  $\bar{E} \approx E_p$ , Eqn (12) becomes

$$\lambda_v \approx 1.88E^{0.78}/E_p = 0.0653E^{0.78}(A/\rho N_v)^{1/2} \quad (\text{in } \text{\AA}) \quad (13)$$

The expressions for  $\lambda$  in Eqn (11) and for  $\lambda_v$  in Eqn (13) are very similar. Both equations show an almost identical dependence on electron energy, and the energy exponents (here, material-independent) fall within the range  $m = 0.706$ – $0.789$  found in the fits of Eqn (7) to our IMFPs described in the previous subsection. Equations (11) and (13) also show the same dependences on material parameters.

For comparison of Eqns (11) and (13) with TPP-2 [Eqns (1)–(6)], we assume that  $E$  is in the range 500–2000 eV so that the terms containing  $C$  and  $D$  in Eqn (1) can be neglected. For simplicity in analysis, we neglect the first and third terms in Eqn (2) so that

$$\beta \approx 0.944/(E_p^2 + E_g^2)^{1/2} \approx 0.944/E_p \quad (14)$$

Equation (1) can then be rewritten

$$\begin{aligned} \lambda &\approx 1.06E/E_p \ln(\gamma E) \\ &= 0.037E(A/\rho N_v)^{1/2}/\ln(\gamma E) \quad (\text{in } \text{\AA}) \end{aligned} \quad (15)$$

If  $\gamma = 0.08 \text{ eV}^{-1}$ , Eqn (15) becomes

$$\gamma \approx 0.045E^{0.76}(A/\rho N_v)^{1/2} \quad (\text{in } \text{\AA}) \quad (16)$$

for the 500–2000 eV range.

The numerator of Eqn (15) shows the same dependences on material parameters as Eqns (11) and (13) but the denominator has an additional material-dependent term. The neglect of the first term in Eqn (2) to yield Eqn (14) is not, however, justified so the TPP-2 dependence on material parameters is more complex than is indicated by Eqn (15) or Eqn (16). It should also be noted that the more exact versions of Eqns (9) and (12) have more complex dependences on material parameters than is indicated here.<sup>13,17</sup>

### AL equation of Seah and Dench

Seah and Dench<sup>18</sup> found that separate sets of AL data for elements, inorganic compounds and organic compounds could be represented by a simple empirical equation

$$\lambda_{AL} = A_i E^{-2} + B_i E^{0.5} \quad (17)$$

where  $A_i$  and  $B_i$  are parameters for each set of data. The expression recommended for elements was

$$\lambda_m = 538E^{-2} + 0.41(aE)^{1/2} \text{ monolayers} \quad (18a)$$

while that for inorganic compounds was

$$\lambda_m = 2170E^{-2} + 0.72(aE)^{1/2} \text{ monolayers} \quad (18b)$$

where  $a$  is the average thickness of a monolayer (in nm), given by

$$a = 10^7(M/\rho nN)^{1/3} \quad (19)$$

where  $n$  is the number of atoms in a molecule (for a compound), and  $N$  is Avogadro's number. The AL (in nm),  $\lambda_n$ , can be obtained from  $\lambda_m$  using

$$\lambda_n = a\lambda_m \quad (20)$$

We note here that, as for Eqn (9), there is no physical basis for Eqn (18) and its parameters other than the energy exponent for the first term.<sup>18</sup>

Seah and Dench introduced a quantity  $\lambda_a$  defined by

$$\lambda_a = \lambda_m a^{-1/2} = \lambda_n a^{-3/2} \quad (21)$$

It was then convenient to propose AL equations that did not have material-dependent terms. Their equation for elements was

$$\lambda_a = 1040E^{-2} + 0.41E^{1/2} \text{ monolayers nm}^{-1/2} \quad (22a)$$

while that for inorganic compounds was

$$\lambda_a = 3990E^{-2} + 0.72E^{1/2} \text{ monolayers nm}^{-1/2} \quad (22b)$$

In deriving Eqns (22a) and (22b), Seah and Dench used average values of  $a$  to determine values for the multiplier of the  $E^{-2}$  term. Equations (22a) and (22b) could then be used as material-independent 'universal curves' for predicting ALs for elements and inorganic compounds, although there was no physical basis given for the different values of  $A_i$  and  $B_i$  for different classes of solids. The use of average values of  $a$  in Eqn (22) would lead to small errors in AL values [compared to Eqn (18)] at energies below  $\sim 50$  eV, outside the range of present interest.

We now compare our IMFP results with the Seah and Dench equations for ALs. This comparison is most easily done with plots of  $\lambda_a$ . Figures 6 and 7 show values of  $\lambda_a$  calculated using Eqns (19) and (21) from IMFP for our group of elements<sup>1</sup> versus electron energy. The solid lines in Figs 6 and 7 show the Seah and Dench equation [Eqn (22a)] for ALs. Figure 8 is a similar plot of  $\lambda_a$  for our group of compounds together with the Seah and Dench expression [Eqn (22b)]; in this plot,  $\lambda_a$  values have been computed using IMFPs calculated from TPP-2.<sup>1</sup> An overall summary plot, similar to Figs 1 and 2, is given in Fig. 9.

It is clear from Figs 6–8 that Eqn (22) agrees only roughly with  $\lambda_a$  values derived from our IMFP data. For electron energies greater than  $\sim 150$  eV, the second term of Eqn (22) dominates and the  $\lambda_a$  values from the Seah and Dench equation show an  $E^{1/2}$  dependence. As indicated earlier, our IMFP values show roughly an  $E^{0.75}$  dependence. Equation (22a) gives a minimum  $\lambda_a$  value for all elements at  $\sim 40$  eV, while Eqn (22b) gives a  $\lambda_a$  minimum value for all inorganic compounds at  $\sim 55$  eV. The energies at which the  $\lambda_a$  values derived from our elemental IMFP have minima in the range 30–125 eV.<sup>1</sup> The corresponding range in  $\lambda_a$  values determined from IMFP calculated from optical data for the group of inorganic compounds is 33–86 eV;<sup>2</sup> the values plotted in Fig. 8 were determined from TPP-2 in the range 50–2000 eV and these values have minima in the 50–60 eV range. We conclude that Eqn (22) does not describe well the material-dependent shapes of the

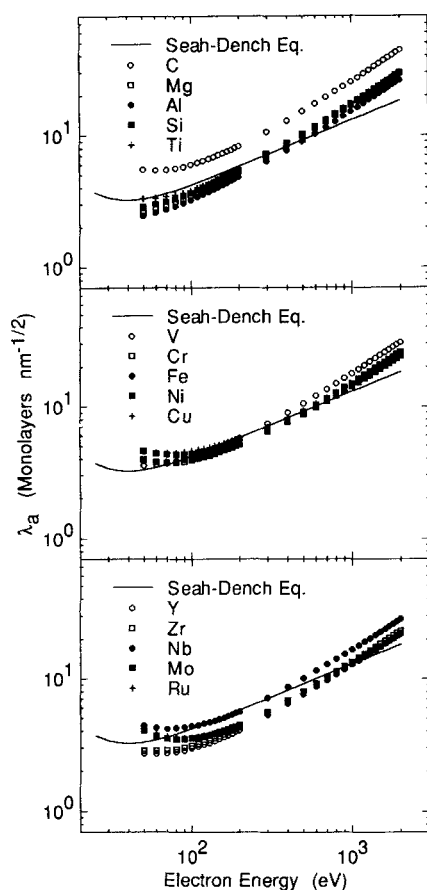


**Figure 6.** Plots of  $\lambda_a$  [defined by Eqn (21)] versus electron energy for groups of elements. The points show values of  $\lambda_a$  calculated from our IMFPs (Ref. 1) and the solid line is the Seah and Dench AL expression [Eqn (22a)].

IMFP-energy curves in the 50–200 eV range, which have been attributed to variations in the shapes of the energy-loss functions from material to material and, at least for free-electron-like solids, to variations in valence-electron density.<sup>1,19</sup> It is also clear from Fig. 3 that TPP-2 does not describe well the shapes of the IMFP-energy curves calculated from optical data in the 50–200 eV range for some elements and compounds, even though the modified Bethe equation [Eqn (1) with four free parameters] can be used to make good fits of the calculated IMFPs, as indicated in Figs 4 and 5. We believe that this deficiency is associated with the large differences in shapes of energy-loss functions from material to material; these differences lead to corresponding differences in the shapes of the IMFP-energy curves.<sup>1,2,20</sup> The variation in shapes of the IMFP-energy curves cannot be represented adequately in terms of simple analytic functions of density, atomic or molecular weight, number of valence electrons per atom or molecule and bandgap energy, such as Eqns (1)–(6).

The summary plot of Fig. 9 shows the material-dependent ranges of the  $\lambda_a$  values. We exclude in this discussion the top-most array of points for carbon in Fig. 9(a) since they appear to be much higher than the points for the other elements. We had previously found that IMFPs calculated from TPP-2 for carbon were 33% (RMS) less than the IMFPs calculated from optical data.<sup>1</sup> This was the largest such deviation and,

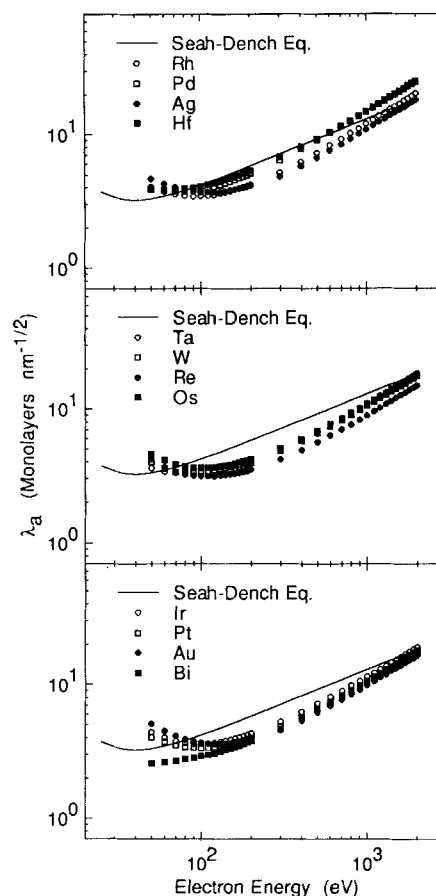


**Figure 7.** Plots of  $\lambda_a$  for additional groups of elements; see caption to Fig. 6.

although we have no definite explanation for this result, we suspect that the density we used for the glassy form of carbon ( $1.8 \text{ g cm}^{-3}$ ) may not be correct. With the exclusion of the data for carbon in Fig. 9(a), the range in elemental values for  $\lambda_a$  at any one energy varies between a factor of 1.6 and a factor of 2.1; this range is only slightly less than the range for IMFP values in Fig. 1. The corresponding range of  $\lambda_a$  values for the inorganic compounds in Fig. 9(b) varies between a factor of 2.0 and a factor of 2.4; this range is substantially greater than the range of IMFP values in Fig. 2(b). We had thought that the  $\lambda_a$  plots of Fig. 9 might show appreciably less material-dependent dispersion than the corresponding plots of Figs 1 and 2(b). The average range in Fig. 9(a) is  $\sim 16\%$  less than the average range in Fig. 1, but the average range in Fig. 9(b) is  $\sim 50\%$  more than the average range in Fig. 2(b).

The material dependences of our TPP-2 for IMFPs and of the Seah and Dench expression for ALs are thus very different. Although Eqns (18) and (22) were derived from experimental AL measurements published prior to 1979, it is now recognized that there are many potential sources of significant systematic error in AL experiments.<sup>6,21</sup> It is also known from detailed studies in recent years that thin films nucleate and grow in different morphological forms. Careful experiments with well-characterized thin films are therefore needed to assess the validity of TPP-2 and of the Seah and Dench expressions for predicting AL material dependences.

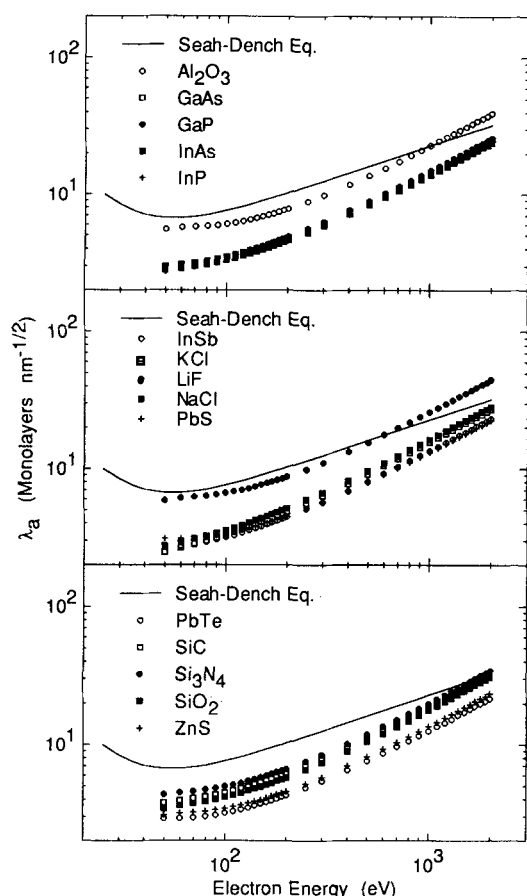


**Figure 8.** Plots of  $\lambda_a$  [defined by Eqn (19)] versus electron energy for groups of inorganic compounds. The points show  $\lambda_a$  values obtained from IMFPs calculated using TPP-2 (Ref. 2). The solid line is the Seah and Dench AL expression [Eqn (22b)].

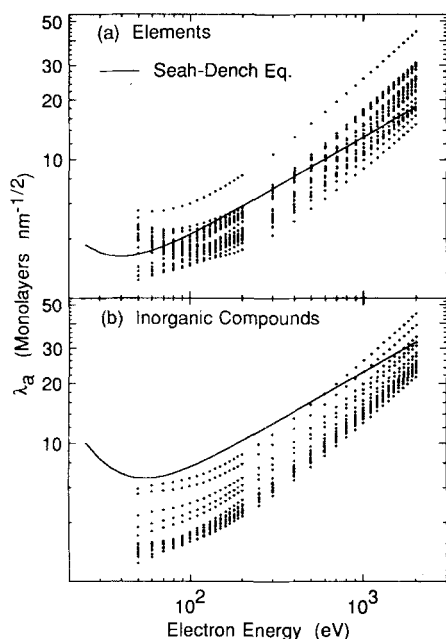


**Figure 9.** Summary plot of  $\lambda_a$  values [defined by Eqn (19)] versus electron energy for (a) the group of 27 elements and (b) the group of 15 inorganic compounds. The  $\lambda_a$  values for the inorganic compounds have been obtained from IMFPs calculated using TPP-2 (Ref. 2).

## RELIABILITY OF PREDICTIVE IMFP AND AL EQUATIONS

The terms IMFP, AL and escape depth are often used interchangeably but each has a separate meaning.<sup>6</sup> The present AL definition has been shown to be inadequate,<sup>22</sup> and it is expected that a definition of a replacement term will be developed shortly. Recent calculations have shown that the attenuation of signal electrons from a substrate does not usually vary exponentially with the thickness of an overlayer film.<sup>22,23</sup> Owing to elastic electron scattering, the IMFP for a given material and electron energy will be systematically larger than the corresponding 'effective' AL by up to ~40%, the difference depending on electron energy, the atomic number of the material and the experimental configuration.

Until recently, it was thought<sup>21</sup> that the AL should be used for matrix corrections in practical surface analyses by AES and XPS. An analysis by Jablonski,<sup>24</sup> however, has shown that the IMFP should be used for AES rather than the AL. Owing to the many experimental difficulties involved in making AL measurements with the needed accuracy,<sup>6,21</sup> we have suggested that our IMFP values and our predictive IMFP formula could be useful for estimating AL values.<sup>1</sup> Alternatively, transport calculations provide a means for determining 'effective' ALs from IMFPs for specified materials and measurement configurations.<sup>23</sup>

A reasonable test for TPP-2 and other predictive equations for IMFPs or ALs is that they give correct analytical results when applied to AES or XPS data obtained from specimens of known composition. Unfortunately, there are many sources of systematic error in practical AES and XPS measurements,<sup>21</sup> and such potential sources of error should be demonstrated to be insignificant in tests of predictive IMFP or AL equations. In addition, it is clear from Fig. 9 that TPP-2 and the Seah and Dench equations, for example, will give similar numerical values for certain materials and for certain energies. A test of two or more IMFP/AL formulae is thus likely to be significant if the AES or XPS measurements are made for materials and electron energies for which the formulae yield different numerical values.

There have been several reports published recently in which comparisons have been made of the analytical accuracy for AES measurements made with Au-Cu alloys and a range of transition-metal silicides.<sup>25</sup> These comparisons have been based on the use of several different formulae for determining ALs, as well as on other parameters such as the choice of sensitivity factors, analytical algorithm, values of other parameters and line-shape changes. While the analytical accuracy in results based on the TPP formula<sup>13</sup> for the 200–2000 eV electron energy range compared favourably with other methods for estimating ALs, the limited number of materials in the measurements made to date and uncertainties in other aspects of the analyses suggest that it is premature to make definitive recommendations at this time. Nevertheless, these comparisons encourage the view that the TPP formula is useful and that, as suggested by Jablonski,<sup>24</sup> the IMFP rather than the AL should be used in AES analyses.

### SENSITIVITY OF IMFPs FROM TPP-2 TO CHOICE OF PARAMETERS

We have previously investigated the extent to which IMFPs calculated from TPP-2 changed when the values of individual parameters were varied in a reasonable range.<sup>1,20</sup> These studies were made for three metals: Al,<sup>1</sup> Cu<sup>20</sup> and Au.<sup>1</sup> The elements Al and Au were chosen because they are perhaps the most extreme examples of free-electron-like and non-free-electron-like metals (as far as their IMFP properties are concerned).<sup>19</sup> Copper was chosen as an example of a transition or noble metal with lower density than for gold. Our evaluations of TPP-2 were made with elemental values for three of the four TPP-2 parameters ( $\rho$ ,  $N_v$ ,  $E_p$  and  $E_g$ ) in a set of calculations and with the fourth varied in a selected range; similar sets of calculations were made as each of the four parameters was chosen for variation.

We found that changes in  $\rho$ ,  $N_v$  and  $E_p$  affected the magnitudes of the computed IMFPs and could also affect (particularly for Cu and Au) the shapes of the IMFP-energy curves in the low-energy (50–200 eV) range. Broad minima in the IMFP-energy curves at low energies (as for Cu and Au) were associated with generally higher values of  $\rho$ ,  $N_v$  and  $E_p$  than those that gave narrower minima (as for Al).

We present here similar sets of calculations for two inorganic compounds:  $\text{Al}_2\text{O}_3$  and GaAs. These compounds were selected because  $\text{Al}_2\text{O}_3$  is a wide-bandgap insulator and has a fairly broad peak in its loss function, while GaAs is a compound semiconductor with a narrower peak in its loss function.<sup>2</sup> The values of parameters needed for the evaluation of TPP-2 for these two compounds are listed in Table 3. By coincidence, the value of  $E_p$  for GaAs is similar to that for Al (15.8 eV) and the value of  $E_p$  for  $\text{Al}_2\text{O}_3$  is close to that for Au (29.9 eV). The densities of these compounds, however, are very different from those of the corresponding metals, and it was thought worthwhile to explore how IMFPs computed from TPP-2 varied with changes in parameter values for these two compounds.

Figures 10–13 show IMFP-energy curves for  $\text{Al}_2\text{O}_3$  and the effects of varying in turn the bulk density  $\rho$ , the number of valence electrons per molecule  $N_v$ , the free-electron plasmon energy  $E_p$  and the bandgap energy  $E_g$ . The solid lines in Figs 10–13 are plots based on the

**Table 3. Parameter values for  $\text{Al}_2\text{O}_3$  and GaAs needed for evaluation of the IMFP predictive formula TPP-2 [Eqns (1)–(6)]**

Parameter	$\text{Al}_2\text{O}_3$	GaAs
$\rho$ ( $\text{g cm}^{-3}$ )	3.97	5.31
$N_v$ (electrons per molecule)	24	8
$E_p$ (eV)	27.8	15.6
$E_g$ (eV)	9.0	1.35
$U$ ( $\text{g cm}^{-3}$ )	0.934	0.294
$\beta$ ( $\text{eV}^{-1} \text{\AA}^{-1}$ )	0.0136	0.0426
$\gamma$ ( $\text{eV}^{-1}$ )	0.0959	0.0829
$C$ ( $\text{\AA}^{-1}$ )	1.12	1.70
$D$ ( $\text{eV \AA}^{-1}$ )	34.0	47.3

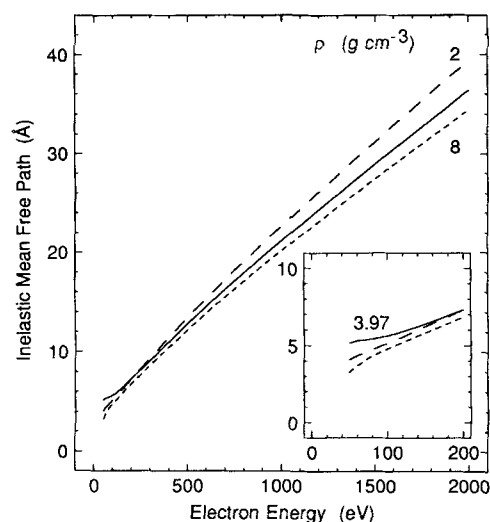


**Figure 10.** Plot of IMFP versus energy for  $\text{Al}_2\text{O}_3$  from TPP-2 (solid line) and of evaluations of TPP-2 [Eqns (1)–(6)] with  $\text{Al}_2\text{O}_3$  parameters except that the bulk density  $\rho$  was varied as shown. The inset shows IMFP values for the 50–200 eV range on an expanded energy scale.

‘correct’ parameter values for  $\text{Al}_2\text{O}_3$  (Table 3) and the other curves indicate the effects of parameter changes.

The IMFP variation in Fig. 10 with change of density is qualitatively similar to that in corresponding plots for Al and Au but the quantitative IMFP changes in Fig. 10 are much less.<sup>1</sup> We also evaluated TPP-2 for  $\rho = 16 \text{ g cm}^{-3}$  but found that the resulting value of  $U$  was 3.77 and thus appreciably outside the range of 0.14–1.55 that was used in the development of TPP-2; as a result, the computed values of  $C$  and  $D$  were negative and the derived IMFP values were considered unreliable (and thus not shown in Fig. 10). Figure 11 shows a decrease in IMFPs as  $N_v$  is increased from 6 to 24 but the IMFPs are larger for  $N_v = 36$  than for  $N_v = 24$ . Similarly, Fig. 12 shows a decrease in IMFPs as  $E_p$  is increased from 10 to 27.8 eV and then an increase for

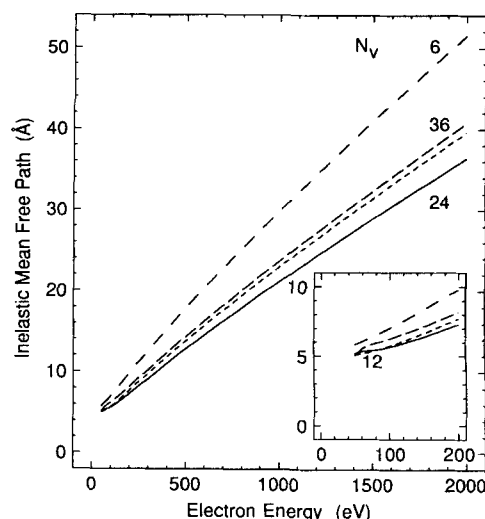


**Figure 11.** Plot of IMFP versus energy for  $\text{Al}_2\text{O}_3$  from TPP-2 (solid line) and of evaluations of TPP-2 with  $\text{Al}_2\text{O}_3$  parameters except that the number of valence electrons per molecule  $N_v$  was varied as shown.



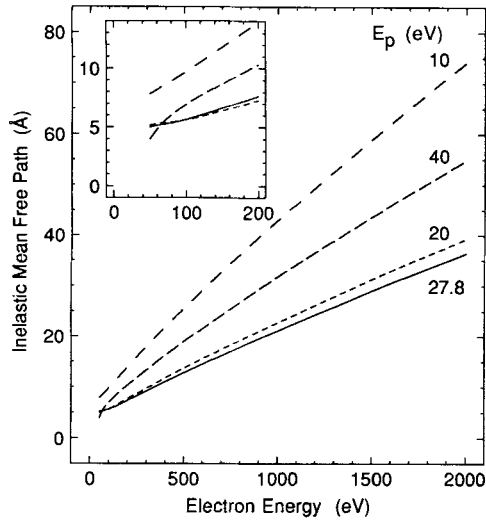


**Figure 12.** Plot of IMFP versus energy for  $\text{Al}_2\text{O}_3$  from TPP-2 (solid line) and of evaluations of TPP-2 with  $\text{Al}_2\text{O}_3$  parameters except that the free-electron plasmon energy  $E_p$  was varied as shown.

$E_p = 40$  eV. IMFP trends of the type presented in Figs 11 and 12 were also found for Al but not for Au.<sup>1</sup> The variation in IMFPs with change of bandgap energy in Fig. 13 is fairly small.

The curves presented in the insets of Figs 10–13 do not show the broad minima found in similar plots for Au.<sup>1</sup> In addition, some of these curves show decreasing IMFPs and increasing curvature of the IMFP–energy plots as the electron energy is reduced from 70 to 50 eV. The increasing curvature for these energies is thought to be non-physical and is probably associated with the relatively large values of  $E_p$  and  $E_g$  and the relatively low values of  $\beta$ ,  $C$  and  $D$  in Eqn (1).

The IMFP plots for GaAs in Fig. 14 show decreasing IMFPs with increasing values of the density; the changes here are larger than for  $\text{Al}_2\text{O}_3$  in Fig. 10. Figures 15 and 16 show a monotonic decrease in IMFP values as  $N_v$  and  $E_p$  are increased. As in Fig. 13 for

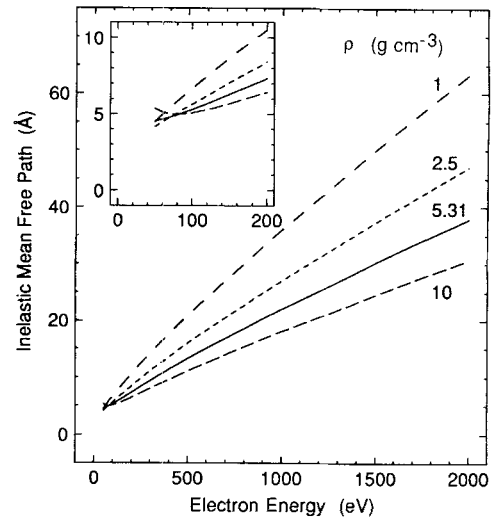


**Figure 14.** Plot of IMFP versus energy for GaAs from TPP-2 (solid line) and of evaluations of TPP-2 with GaAs parameters except that the bulk density  $\rho$  was varied as shown.

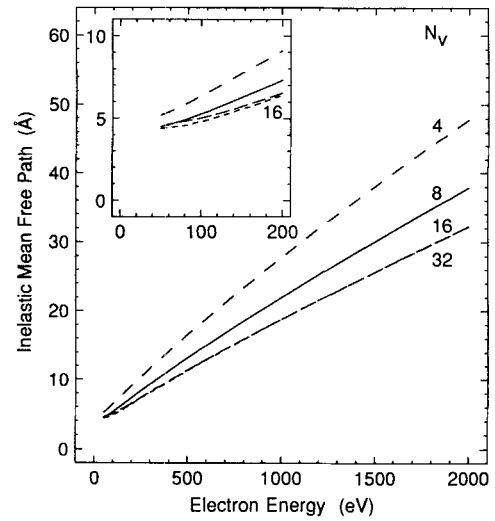


**Figure 15.** Plot of IMFP versus energy for GaAs from TPP-2 (solid line) and of evaluations of TPP-2 with GaAs parameters except that the number of valence electrons per molecule  $N_v$  was varied as shown.

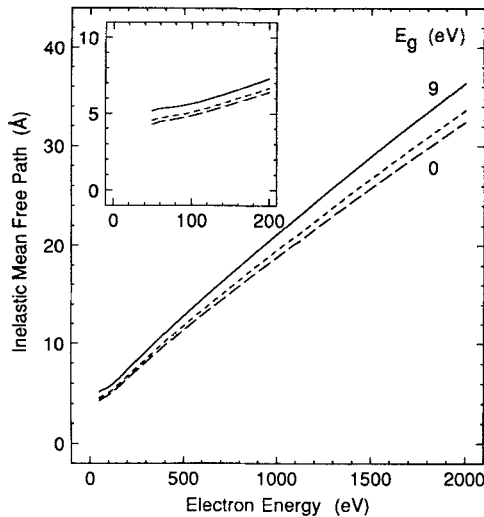


**Figure 13.** Plot of IMFP versus energy for  $\text{Al}_2\text{O}_3$  from TPP-2 (solid line) and of evaluations of TPP-2 with  $\text{Al}_2\text{O}_3$  parameters except that the bandgap energy  $E_g$  was varied as shown. The intermediate curve is for  $E_g = 5$  eV.

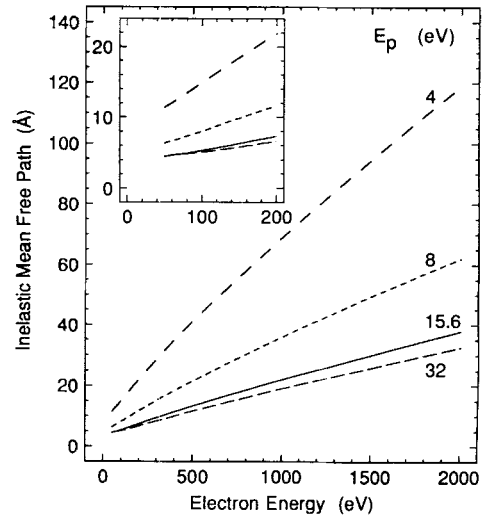


**Figure 16.** Plot of IMFP versus energy for GaAs from TPP-2 (solid line) and of evaluations of TPP-2 with GaAs parameters except that the free-electron plasmon energy  $E_p$  was varied as shown.

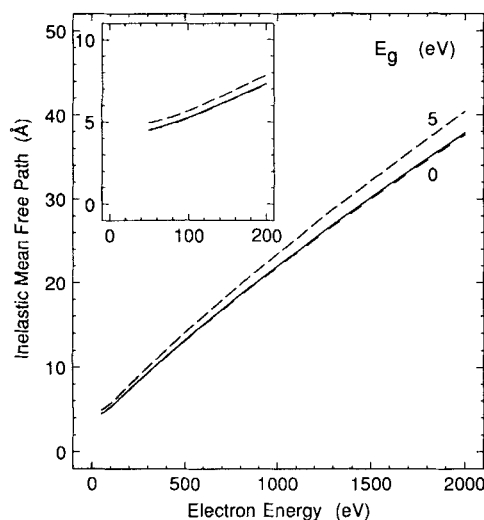


**Figure 17.** Plot of IMFP versus energy for GaAs from TPP-2 (solid line) and of evaluations of TPP-2 with GaAs parameters except that the bandgap energy  $E_g$  was varied as shown. For GaAs,  $E_g = 1.35$  eV.

$\text{Al}_2\text{O}_3$ , relatively small changes in IMFP occur with variation of  $E_g$  for GaAs in Fig. 17.

We point out that the IMFPs plotted in Figs 10–17 cover a wide but realistic range in values for the TPP-2 parameters. In these as well as the similar simulations for Al, Cu and Au,<sup>1,20</sup> TPP-2 has been found to be robust. In the use of TPP-2 for any specific material, it is suggested that TPP-2 be evaluated with different reasonable choices of parameters (e.g. for  $N_v$ ), should there be doubt as to the correct value to be employed, in order to determine the sensitivity of the IMFP to the parameter choice.

## SOURCES OF UNCERTAINTY IN IMFPs

We have previously summarized sources of uncertainty in our calculations of IMFPs from optical data.<sup>1</sup> These uncertainties are of two general types: uncertainties associated with the IMFP algorithm, and its application to a wide range of materials for quantitative AES and XPS; and uncertainties associated with the optical data for a particular material. We now discuss these two types of uncertainty and then add remarks about uncertainties of TPP-2.

### Uncertainties in IMFPs for AES and XPS

We consider first uncertainties associated with the IMFP algorithm.<sup>3</sup> The algorithm is based on the statistical approximation, with which it is assumed that the inelastic scattering of an electron at any point in a solid can be approximated by the scattering appropriate to a free-electron gas with the electron density found at that point. The inelastic scattering is described by the Lindhard dielectric function,<sup>4</sup> which depends on energy loss, momentum transfer and electron density. The statistical model is modified in such a way that the values of the

energy-loss function obtained from experimental optical data (which correspond to inelastic scattering with zero momentum transfer) are reproduced by the theory. This model provides a physically plausible dependence of the inelastic scattering probability on momentum transfer through the use of the Lindhard dielectric function. While this particular dependence may not be correct in detail, it is based on a physically reasonable model and we do not currently have a better approach.

Our algorithm neglects exchange and correlation effects that are expected to be more significant at low energies ( $<200$  eV). Ashley<sup>26</sup> has treated the effects of exchange on the IMFP in an approximate way and found that the resultant IMFP values were larger (by up to 40% at 40 eV) than those for which exchange was ignored. Another plausible treatment,<sup>27</sup> however, has found corrections of the opposite sign. More detailed assessments of exchange and correlation effects remain to be made.

We also expect that the actual band structure of a solid should be considered if it differs appreciably from that for a free-electron-like material. Such considerations are likely to be important for transition metals and for very low electron energies ( $<50$  eV). Cailler *et al.*<sup>28</sup> have reviewed various methods for the calculation of IMFPs.

Our IMFP calculations are for bulk solids. For quantitative AES and XPS, however, the detected electrons of interest originate in a near-surface region and traverse the solid/vacuum interface. It is known that the inelastic scattering modes near a surface or interface are different from the corresponding bulk materials.<sup>29</sup> Although the cross-sections for inelastic scattering by bulk and surface processes depend on proximity to the surface and other parameters, there is an approximate cancellation in the increase of the bulk scattering cross-section and decrease of the surface scattering cross-section with distance from the surface.<sup>29</sup> Effects of this type have been investigated by Yubero and Tougaard<sup>30</sup> for reflection electron energy-loss spectroscopy. It is therefore possible that the energy dependence of our calculated bulk IMFPs may need to be modified to account for surface effects for applications in quantitative AES and XPS. Any such modifications would presumably be more important for low electron energies and for near-grazing take-off angles, although we suspect that the corrections are not significant for electron energies above  $\sim 200$  eV and for take-off angles (measured with respect to the plane of the surface) greater than  $\sim 45^\circ$ .<sup>31</sup>

It is difficult for us to estimate the magnitudes of the uncertainties discussed above. The neglect of correlation and exchange effects will be most significant for electron energies below  $\sim 200$  eV. The corrections associated with surface excitations in AES and XPS applications are also believed to be significant for energies below  $\sim 200$  eV. We therefore conclude that the dependence of the calculated IMFPs on energy is likely to be reliable for electron energies above  $\sim 200$  eV but corrections at lower energies could be required. The uncertainty associated with the IMFP algorithm has been estimated to be  $\sim 10\%$  for free-electron-like materials and for energies above 200 eV; the uncertainty for other materials and at lower energies is expected to be larger, but its magnitude is difficult to estimate.<sup>1,13</sup> Neverthe-

less, because we have used the same algorithm in a consistent way in IMFP calculations for the group of 27 elements, we believe that the relative IMFPs are known with greater confidence than the absolute values, i.e. we believe that our set of IMFP results can be analysed usefully for determining IMFP dependences on material parameters (e.g. at a constant energy) and on electron energy (for different materials).

### Uncertainties of the optical data

For any one material, the accuracy of a calculated IMFP will depend on the accuracy of the experimental optical data used in the calculation. We have therefore analysed the internal consistency of sets of optical data for our groups of elements and inorganic compounds with two powerful sum rules.<sup>2,20</sup> These sum rules were satisfied typically to an average RMS uncertainty of  $\sim 10\%$  for the group of elements<sup>13</sup> and to  $\sim 18\%$  for the group of inorganic compounds.<sup>2</sup> The sum rules, however, involve integrations of different frequency moments of the energy-loss function  $Im[-1/\epsilon(\omega)]$ , where  $\epsilon(\omega)$  is the complex frequency-dependent dielectric constant, over a large frequency range. The calculated IMFPs are mainly determined by values of the energy-loss function in the photon energy range of 5–300 eV.<sup>20</sup>

The sum rules give useful information on the overall consistency of the optical data, and we assume that the accuracy of the optical data between 5 and 300 eV is roughly the same. It is possible, however, that large errors in the sum-rule tests could be due to inaccuracies in the optical data outside the range 5–300 eV. It is also possible that a sum-rule error might be found to be small but that potential errors in the 5–300 eV range could be negated largely in the integrations by errors of opposite sign at other photon energies.

We note that there were gaps in the available optical data for some of the materials for which we have made IMFP calculations.<sup>1,2</sup> These gaps generally occurred for photon energies between  $\sim 30$  and 100 eV. In these cases, we made interpolations based on atomic photoabsorption data. The interpolations may not be correct in detail for the corresponding solids, particularly in the vicinity of absorption thresholds, but the interpolations are considered to contribute a relatively small uncertainty to the calculated IMFPs on account of the integration of the loss function.

Our tabulated IMFPs for each element<sup>1</sup> would therefore be expected to have an individual uncertainty associated with the average of the two sum-rule errors for that element.<sup>13,20</sup> Since the sum-rule errors for the compounds were generally much larger than for the elements, we found that we could obtain IMFPs more reliably with our TPP-2 formula.<sup>2</sup>

### Uncertainties of the TPP-2 formula

The TPP-2 formula is based on the Bethe<sup>5</sup> equation for inelastic electron scattering in matter, although expressions for the four parameters were determined empirically.<sup>1</sup> Since TPP-2 is based on a physical model, it is reasonable to believe that it is broadly applicable to all classes of solids. Further refinements may be made in

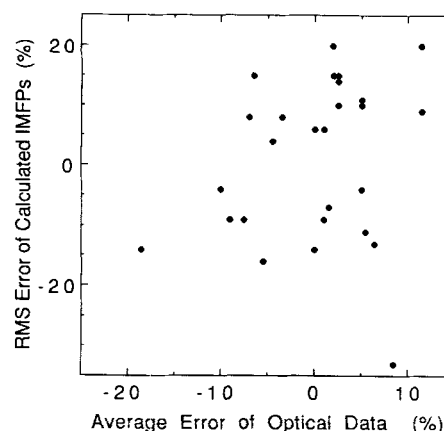


**Figure 18.** Plot of the RMS errors in comparisons of IMFP values calculated from optical data with those expected from TPP-2 for our group of elements (Ref. 1) versus the average of the errors in the optical data as derived from two sum rules (Ref. 13).

the future, but for the present it appears to provide a reasonable description of the IMFP dependences on material parameters and on electron energy for the group of 27 elements.

The RMS difference between elemental IMFPs calculated from optical data and those determined from TPP-2 was  $\sim 13\%$ .<sup>1</sup> This RMS difference is not appreciably greater than the average RMS uncertainty of the optical data ( $\sim 10\%$ ) derived from the sum-rule tests. Figure 18 is a plot of the RMS error in comparisons of IMFPs calculated from optical data for our group of elements<sup>1</sup> with those expected from TPP-2 versus the average error of the optical data (as determined from our sum rule evaluations<sup>13</sup>). No obvious correlation is apparent, unlike the result of a similar plot for our group of inorganic compounds.<sup>2</sup> Our TPP-2 formula thus appears to be a useful means of 'averaging out' the sum-rule errors for any one material. Substantial contributions to the 13% RMS difference between elemental IMFPs obtained from optical data and those computed from TPP-2 arise for electron energies between 50 and 200 eV (Fig. 3). As discussed previously, a simple analytical formula such as TPP-2 cannot be expected to represent adequately the effects of detailed differences in the shapes of the energy-loss functions for different materials. Such differences are more pronounced for IMFP calculations in the 50–200 eV range than at higher energies.<sup>1</sup>

The generally greater deviations of the ratios plotted in Fig. 3 from unity in the 50–200 eV range (compared to higher energies) indicate that TPP-2 has lower accuracy at these low energies. This conclusion is also reinforced by the computed shapes of the IMFP-energy curves in the 50–200 eV range for some variations of parameters in Figs 10–12 that appear to have unphysical shapes.

We have previously considered whether a simpler or more accurate expression than TPP-2 might be derived for the prediction of IMFPs.<sup>20</sup> The magnitude of an IMFP calculated for a material from TPP-2 at some energy greater than 200 eV is largely determined by the product  $\beta E_p^2$  [i.e. for energies where the terms involving  $C$  and  $D$  in Eqn (1) are small compared to  $\beta \ln(\gamma E)$ ]. Our empirical values<sup>1</sup> of  $\beta$  for each material are  $\sim 10\%$  larger than the asymptotic values  $\beta_{\text{opt}}$  expected when

the electron energy is sufficiently high ( $> 2000$  eV). The value of  $\beta_{\text{opt}}$  can be calculated from<sup>20</sup>

$$\beta_{\text{opt}} = M_{\text{tot}}^2 / 28.8 N_v \quad (\text{eV}^{-1} \text{\AA}^{-1}) \quad (23)$$

where  $M_{\text{tot}}^2$  is the square of the dipole matrix element for all possible inelastic scattering processes, and is defined by

$$M_{\text{tot}}^2 = 2R/\pi \hbar^2 \Omega_p^2 \int_0^{\Delta E_{\text{max}}} \times \text{Im}[-1/\varepsilon(\Delta E)] d(\Delta E) \quad (24)$$

for  $\Delta E_{\text{max}} = \infty$ . In Eqn (24),  $R$  is the Rydberg energy (13.606 eV),  $\Omega_p = (4\pi n_a e^2/m)^{1/2}$ ,  $n_a = N\rho/M$  is the density of atoms or molecules and  $\Delta E = \hbar\omega$  is the excitation energy in an inelastic scattering event. For atoms,  $M_{\text{tot}}^2$  is related to summations of the position vectors of atomic electrons, and there are systematic trends in plots of  $M_{\text{tot}}^2$  versus  $Z$ .<sup>32</sup> Nevertheless, there are no known relationships involving  $M_{\text{tot}}^2$  for solids and simple material parameters. Without such a relationship, it is unlikely that a simple but improved IMFP formula can be developed for energies in the range 200–2000 eV. Improvements at lower energies will depend on the development of new understanding and improved parameterizations for describing inelastic electron scattering in materials at such energies.

## SUMMARY

We have presented additional evaluation of IMFPs for 27 elements and 15 inorganic compounds presented in papers II and III of this series and of the IMFP predictive formula TPP-2 described in paper II.

We have found that our computed IMFPs can be fitted to the simple power-law dependence on electron energy proposed by Wagner *et al.*<sup>8</sup> [Eqn (7)] for energies between 500 and 2000 eV. The energy exponent is in the range 0.706–0.789 for our materials. While the average value of this exponent (0.75) could provide a reasonable guide to the energy dependence of the IMFP in the 500–2000 eV range, we point out that our earlier TPP formula<sup>13</sup> (also with two parameters) provides a superior fit to the IMFP data over the 200–2000 eV range and that the present TPP-2 formula (with four parameters) is better over the 50–2000 eV range. Moreover, unlike the situation for the TPP and TPP-2 formulae, Eqn (7) is an empirical relationship and there is no physical basis for the form or how the two parameters may vary with material.

The two IMFP formulae developed by Szajman *et al.*<sup>15</sup> and by Ashley<sup>17</sup> show very similar dependences of the IMFP on energy to those we have found with TPP-2 in the 500–2000 eV range. There are similarities in the dependences on material parameters but differences in detail.

We have compared our computed IMFPs with AL values determined from the empirical Seah and Dench equations.<sup>18</sup> In general, there is only a rough correspondence. For electron energies above 200 eV, the ALs from the Seah and Dench equations show an  $E^{1/2}$  dependence on energy while our IMFPs exhibit close to an  $E^{0.75}$  variation (for energies above 500 eV). In the

50–200 eV energy range there are substantial variations in the shapes of the IMFP–energy curves for different materials that are not reflected in the Seah and Dench AL expressions. There are also differences in the dependences on material parameters; experimental checks of these different dependences would be very desirable.

Several studies have been published recently in which comparisons of quantitative analyses were made based on AES measurements with Au–Cu alloys and transition-metal silicides and with different methods for the matrix corrections.<sup>25</sup> Jablonski<sup>24</sup> has pointed out that the IMFP rather than the AL should be used in the matrix correction for AES measurements. The recent comparisons indicate that the TPP formula for IMFPs between 200 and 2000 eV performs as well as, or better than, other IMFP or AL expressions.

We have evaluated TPP-2 through IMFP calculations for  $\text{Al}_2\text{O}_3$  and GaAs as one parameter in turn ( $\rho$ ,  $N_v$ ,  $E_p$  or  $E_g$ ) was varied in some physically reasonable range about the true value for each compound. These simulations indicate that TPP-2 is robust, although in some instances the shapes of the IMFP–energy curves in the 50–70 eV range were judged to be not physically reasonable. In applications with TPP-2, it is suggested that IMFPs should be computed for some reasonable range of parameter values should there be doubt as to the correct value of any parameter (e.g.  $N_v$ ).

Finally, we have presented a summary of sources of uncertainty in our computed IMFPs. Approximations made in developing the IMFP algorithm<sup>3</sup> have been estimated to lead to uncertainties in the IMFP values of  $\sim 10\%$  for free-electron-like materials and for energies above 200 eV; for other materials and for lower energies, the uncertainties are expected to be larger. Our IMFPs are for bulk solids and corrections due to surface effects are likely below 200 eV for applications in quantitative AES and XPS. The IMFP results for any one material will have additional uncertainty associated with the experimental optical data used in the calculations; the average RMS uncertainty of this type has been estimated from sum-rule tests of the optical data to be  $\sim 10\%$  for our group of elements. Larger uncertainties in the optical data for our group of inorganic compounds led to the recommendation that IMFPs be determined from TPP-2 for these materials.<sup>2</sup>

Our TPP-2 predictive IMFP formula is based on the Bethe equation for inelastic electron scattering and is therefore expected to be useful for all types of solids. This formula provides a convenient and useful means for estimating IMFPs in materials for which IMFP calculations have not been made. The RMS difference between elemental IMFPs calculated from optical data and those determined from TPP-2 is  $\sim 13\%$ ,<sup>1</sup> although it should be noted that the deviations in the 50–200 eV range are generally greater than those for higher energies.

We find the TPP-2 formula for predicting IMFPs to be useful and robust in the range of parameter space from which it was developed. This formula is based on IMFP calculations<sup>1</sup> for values of the parameter  $U$  ranging between 0.14 and 1.55 and for electron energies between 50 and 2000 eV. We recommend that TPP-2 should not be used for  $U$  values and energies outside the quoted ranges.

## REFERENCES

1. S. Tanuma, C. J. Powell and D. R. Penn, *Surf. Interface Anal.* **17**, 911 (1991), paper II in this series.
2. S. Tanuma, C. J. Powell and D. R. Penn, *Surf. Interface Anal.* **17**, 927 (1991), paper III in this series.
3. D. R. Penn, *Phys. Rev. B* **35**, 482 (1987).
4. J. Lindhard and M. Scharff, *K. Dan. Vidensk. Selsk. Mat.-Fys. Medd.* **27**, no. 15 (1953); J. Lindhard, M. Scharff and H. E. Schiott, *K. Dan. Vidensk. Selsk. Mat.-Fys. Medd.* no. 14 (1963); D. Pines, *Elementary Excitations in Solids*, p. 144. W. A. Benjamin, New York (1963).
5. H. Bethe, *Ann. Phys.* **5**, 325 (1930).
6. C. J. Powell, *J. Electron Spectrosc.* **47**, 197 (1988).
7. C. J. Powell, in *Quantitative Surface Analysis of Materials*, ed. by N. S. McIntyre, ASTM STP 643, p. 5. American Society for Testing and Materials, Philadelphia (1978).
8. C. D. Wagner, L. E. Davis and W. M. Riggs, *Surf. Interface Anal.* **2**, 53 (1980).
9. C. J. Powell, *Surf. Interface Anal.* **7**, 256 (1985).
10. H. Ebel, M. F. Ebel, P. Baldauf and A. Jablonski, *Surf. Interface Anal.* **12**, 172 (1988).
11. M. F. Ebel, H. Ebel, C. Puchberger and R. Svagera, *J. Electron Spectrosc.* **57**, 357 (1991).
12. J. C. Ashley and C. J. Tung, *Surf. Interface Anal.* **4**, 52 (1982).
13. S. Tanuma, C. J. Powell and D. R. Penn, *Surf. Interface Anal.* **11**, 577 (1988), paper I in this series.
14. C. J. Powell, *Surf. Interface Anal.* **7**, 263 (1985).
15. J. Szajman, J. Liesegang, J. G. Jenkin and R. C. G. Leckey, *J. Electron Spectrosc.* **23**, 97 (1981).
16. J. Szajman and R. C. G. Leckey, *J. Electron Spectrosc.* **23**, 83 (1981).
17. J. C. Ashley, *J. Electron Spectrosc.* **28**, 177 (1982).
18. M. P. Seah and W. A. Dench, *Surf. Interface Anal.* **1**, 2 (1979).
19. S. Tanuma, C. J. Powell and D. R. Penn, *J. Vac. Sci. Technol. A* **8**, 2213 (1990).
20. S. Tanuma, C. J. Powell and D. R. Penn, *Acta Phys. Polon.* **81**, 169 (1992).
21. C. J. Powell and M. P. Seah, *J. Vac. Sci. Technol. A* **8**, 735 (1990).
22. A. Jablonski and H. Ebel, *Surf. Interface Anal.* **11**, 627 (1988); W. H. Gries and W. S. M. Werner, *Surf. Interface Anal.* **16**, 149 (1990).
23. A. Jablonski, *Surf. Sci.* **188**, 164 (1987); A. Jablonski, *Surf. Interface Anal.* **14**, 659 (1989); A. Jablonski and S. Tougaard, *J. Vac. Sci. Technol. A* **8**, 106 (1990); W. S. M. Werner, W. H. Gries and H. Stori, *J. Vac. Sci. Technol. A* **9**, 21 (1991); Z.-J. Ding, PhD Thesis, Osaka University (1990); W. S. M. Werner, W. H. Gries and H. Stori, *Surf. Interface Anal.* **17**, 693 (1991); Y. F. Chen, C. M. Kwei and C. J. Tung, *J. Phys. D* **25**, 262 (1992); W. S. M. Werner, *Surf. Interface Anal.* **18**, 217 (1992).
24. A. Jablonski, *Surf. Interface Anal.* **15**, 559 (1990).
25. S. Tanuma, T. Sekine, K. Yoshihara, *et al.*, *Surf. Interface Anal.* **15**, 466 (1990); A. I. Zagorenko and V. I. Zaporozhenko, *Surf. Interface Anal.* **17**, 237 (1991); Th. Wirth, *Surf. Interface Anal.* **18**, 3 (1992).
26. J. C. Ashley, *J. Electron Spectrosc.* **46**, 199 (1988).
27. D. R. Penn, *Phys. Rev. B* **22**, 2677 (1980).
28. M. Cailler, J. P. Ganachaud and D. Roptin, in *Advances in Electronics and Electron Physics*, ed. by P. W. Hawkes, Vol. 61, p. 161. Academic Press, New York (1983).
29. R. H. Ritchie, *Phys. Rev.* **106**, 874 (1957).
30. F. Yubero and S. Tougaard, *Phys. Rev. B* **46**, 2486 (1992).
31. C. J. Powell, *Rev. Sci. Instrum.* **44**, 1031 (1973); S. Tougaard and I. Chorkendorff, *Phys. Rev. B* **35**, 6570 (1987); J. C. Ingram, K. W. Nebesny and J. E. Pemberton, *Appl. Surf. Sci.* **44**, 279 (1990).
32. M. Inokuti, J. L. Dehmer, T. Baer and J. D. Hanson, *Phys. Rev. A* **23**, 95 (1981).